

# PCCP

Accepted Manuscript



This is an *Accepted Manuscript*, which has been through the Royal Society of Chemistry peer review process and has been accepted for publication.

*Accepted Manuscripts* are published online shortly after acceptance, before technical editing, formatting and proof reading. Using this free service, authors can make their results available to the community, in citable form, before we publish the edited article. We will replace this *Accepted Manuscript* with the edited and formatted *Advance Article* as soon as it is available.

You can find more information about *Accepted Manuscripts* in the [Information for Authors](#).

Please note that technical editing may introduce minor changes to the text and/or graphics, which may alter content. The journal's standard [Terms & Conditions](#) and the [Ethical guidelines](#) still apply. In no event shall the Royal Society of Chemistry be held responsible for any errors or omissions in this *Accepted Manuscript* or any consequences arising from the use of any information it contains.

## COMMUNICATION

## Mesoporous BN and BCN Nanocages with High Surface Area and Spherical Morphology

Cite this: DOI: 10.1039/x0xx00000x

Ulka Suryavanshi,<sup>b</sup> Veerappan V. Balasubramanian,<sup>b</sup> Kripal S. Lakhi,<sup>a</sup> Gurudas P. Mane,<sup>b</sup> Katsuhiko Ariga,<sup>b</sup> Jin-Ho Choy,<sup>c</sup> Dae-Hwan Park<sup>c</sup>, Abdullah Al-Enizi,<sup>d</sup> and Ajayan Vinu<sup>a,b\*</sup>

Received 00th January 2012,  
Accepted 00th January 2012

DOI: 10.1039/x0xx00000x

www.rsc.org/

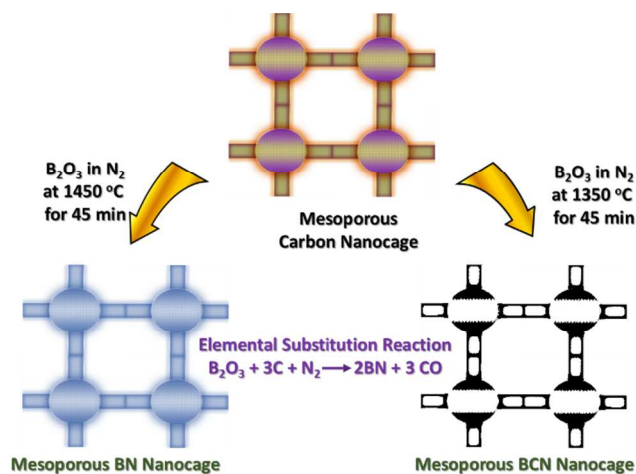
**Novel mesoporous BN and BCN materials with cage type porous structure and spherical morphology have been synthesized using carbon nanocage with 3D porous structure as a template via elemental substitution method at a low synthesis temperature. The obtained materials exhibit a large specific pore volume with uniform pore size distribution and the specific surface area ranging from 945 to 1023 m<sup>2</sup>/g.**

The hexagonal boron nitride (BN) is an insulator with a wide band gap of 5.5 eV and has a graphite type structure which is comprised of alternating boron and nitrogen atoms that are bound by strong covalent bonds.<sup>1</sup> This fascinating electronic structure of BN offers excellent properties such as chemical inertness, high melting point, low density, high thermal conductivity, high oxidation resistance at high temperatures, strong luminescence in the UV range, and optical transparent,<sup>1</sup> which make BN an interesting material and available for many applications such as high temperature devices or furnaces, and mold release liners.<sup>2</sup> Moreover, the surface of BN is extremely hydrophobic in nature that can prevent moisture condensation and keep its surface stable even at a high temperature or in a chemically active environment.<sup>3</sup> It is also expected that the incorporation of carbon atoms into hexagonal boron nitride may afford added hardness and change the electronic properties from insulator to semiconductor and the surface charge of the materials. Although these materials offer interesting properties, the textural parameters of the materials such as specific surface area are quite inferior to other nanomaterials which limit their applications including catalysis.

Therefore, much efforts have been devoted to increase the surface area of the nanomaterials by simply controlling the morphology.<sup>4-7</sup> For example, nanomaterials with spherical morphology exhibit much higher surface area than the nanomaterials with other morphologies and can serve as containers for encapsulation, delivery of drugs, development of artificial cells, and protection of biologically active agents. However, the synthesis of BN and BCN

with spherical morphology and high surface area is quite difficult and challenging.<sup>9-12</sup> Tang et al.<sup>8</sup> tried to fabricate the BN spherical particles by a chemical vapor deposition (CVD) route but the specific surface area of the BN is less than ~20 m<sup>2</sup> g<sup>-1</sup>. Attempts have also been made to modify the surface structure of BN spheres in order to increase the surface area. However, the surface area was merely increased to 22 m<sup>2</sup> g<sup>-1</sup>.<sup>13</sup>

Vinu et al. and Bois et al. independently realized this opportunity and solved the problem by introducing the mesoporosity<sup>14</sup> in the BN and BCN matrix through nanohard-templating approach although the methods adopted by these two groups are quite different.<sup>15,16</sup> Vinu et al. used the combined strategy of elemental substitution and nanotemplating (nanoporous carbon) for the fabrication of mesoporous BN and BCN.<sup>16</sup> However, the adopted technique and the templated material could increase the surface area of the BN only upto 500 m<sup>2</sup>/g because of the 1D structure of the template. In addition, the morphology of the materials is neither spherical nor



uniform.

**Scheme 1** Synthesis of mesoporous BN and BCN nanocages

In this study, we present a simple approach to introduce not only the spherical morphology and high specific surface area in BN and BCN but also cage type 3D porous structure by elemental substitution method using 3D mesoporous carbon nanocage with spherical morphology as a template at relatively low synthesis temperature.<sup>17</sup> By taking the advantage of the 3D structure, high surface area, spherical morphology, cage type porous structure and thin carbon walls of the template, we can replicate the structural features of the template into BN and BCN by a simple elemental substitution of B, and N in the carbon wall. The prepared materials exhibit the spherical morphology similar to that of the template, large pore volume, and the surface area ranging from 945 to 1023 m<sup>2</sup>/g.

The materials were fabricated via elemental substitution reaction using mesoporous carbon nanocage with uniform pore diameter as a template<sup>17</sup> and boron trioxide as a boron source. General synthesis procedures for mesoporous BN (MBN) and mesoporous BCN (MBCN) is as follows: 40 mg of mesoporous carbon nanocage template was placed above a cleaned graphitic crucible containing 400 mg of B<sub>2</sub>O<sub>3</sub> in a flow of nitrogen (inlet flow 3 L/min) for 45 min at 1350 °C for MBCN and 1450 °C for MBN. The heating was carried out in a vertical induction furnace where vapours of B<sub>2</sub>O<sub>3</sub> have been allowed to react with the template. The reaction temperature was monitored using an optical pyrometer with the accuracy of ±10 °C. After the reaction, the excess amount of the unreacted B<sub>2</sub>O<sub>3</sub> was deposited on the graphite crucible. MBN and MBCN were collected from the graphite dish with many small holes placed above the B<sub>2</sub>O<sub>3</sub>. The synthesis of these materials is highly reproducible and almost 100% conversion of carbon nanocage into MBN can be easily achieved.

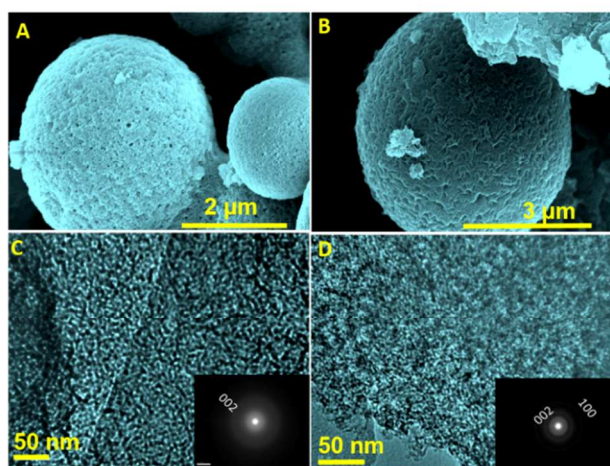


**Fig. 1** HRSEM and HRTEM images of MBN and MBCN nanocages (A and C: MBN; B and D: MBCN)

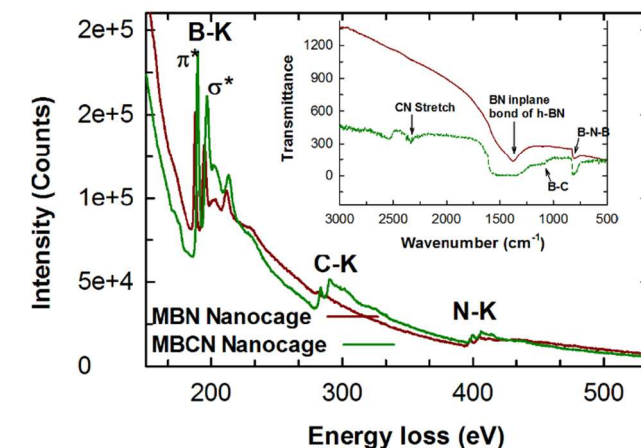
The XRD patterns of the MBN and MBCN (see Fig S1) show two diffraction peaks at 2 $\theta$  of around 26° and 43°, which correspond to the (002) and (100) diffraction lines of BN. These results reveal the formation of the turbostratic phase of BN which has a semi-crystalline structure and is analogous to turbostratic carbon black. This means that the BN layers are stacked together and parallel to each other, and retain 2D ordering in the wall structure of BN. In addition, the domain size of the corresponding crystallites in the wall structure is very small. The morphology of the BN and BCN nanocages is shown in Fig. 1A and 1B. These images clearly show the formation of microspheres (around 1-3  $\mu$ m) with interconnected

mesoporous channels, demonstrating a perfect elemental substitution of B and N in place of C in the template (Fig. 2S). It should also be noted that the surface of the MBN and MBCN nanocages is quite rough.

The ordered mesoporosity generated from the carbon nanocage was confirmed by HRTEM, which clearly show the presence of 3D interconnected mesopores throughout of the spherical particles (Fig. 1C and 1D). The selected area electron diffraction pattern of the MBCN shows an intense row of (002) while only a partial crystallinity is observed for MBN. These results indicate that the mesoporous carbon walls, which are previously amorphous, are transformed into crystalline BCN walls after the substitution reaction. It is interesting to note that the synthesis temperature used for the formation of the BN (1450 °C) and BCN (1350 °C) nanocages is much lower than that of the previously reported method (1750°C).<sup>16</sup> This could be due to the fact that the wall thickness and the density of the carbon nanocage are much smaller than that of the templates used in the previous reports which enhance the substitution reaction at comparatively low temperature.

The elemental composition, the purity, and the structure of mesoporous BN and BCN are analyzed by electron energy loss (EEL) spectroscopy and the results are given in Fig. 2. The EEL spectrum of BN shows only B and N characteristics of K edges while BCN exhibits K-shell excitation edges of boron, carbon and nitrogen. The *sp*<sup>2</sup> bonding nature of the B and N hexagonal layers in BN is also confirmed by the shape and the presence of sharp  $\pi^*$  peaks and  $\sigma^*$  bands.<sup>19,20</sup> The BN sample clearly shows the 1s $\rightarrow\pi^*$  and 1s $\rightarrow\sigma^*$  transitions which are the characteristics of hexagonal BN layered materials, confirming that the walls of MBN are composed of stacked BN layers.<sup>19,20</sup>

Interestingly, the intensity of the B-K shell edge is much higher than that of the N-K excitation edge, which may be attributed to the fact that the densities of empty  $\pi^*$  states of B and N are quite different due to their distinct valence states.<sup>19,20</sup> This is also one of the features of the *sp*<sup>2</sup> hybridized material and can be the finger print of the hexagonal layered BN.<sup>19,20</sup> The absence of the O-K shell excitation edges above 540 eV also confirms the purity of the MBN nanocage structure.<sup>19</sup> On the other hand, MBCN displays K-shell excitation edges of C, B and N, revealing the incorporation of the C atoms in the BN layers. It is also worth noting that fine structure of B-K edges displays a strong  $\pi^*$  peak than  $\sigma^*$  in both MBN and MBCN which indicates that the materials are highly crystalline in nature.<sup>19,20</sup> B:N ratio calculated from EELS spectra is nearly 1:0.9 while B:C:N ratio for MBCN is 2:1:1. The absence of the carbon signal in mesoporous BN sample confirms the purity of the sample even when the reaction temperature was reduced from 1750 to 1450

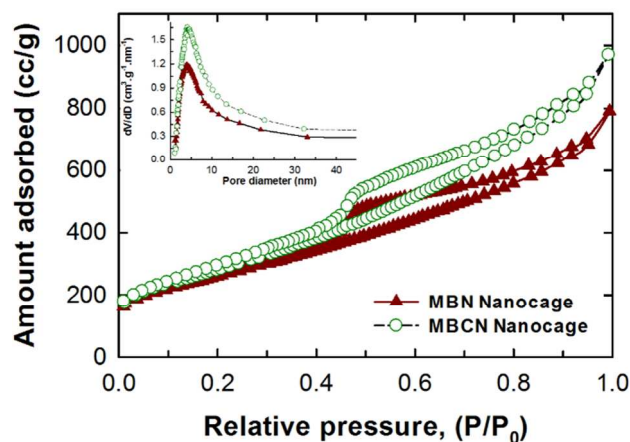


°C.

Fig. 2 EEL spectrum of MBN and MBCN nanocages (inset: FT-IR spectrum of the same samples)

The formation of MBN and MBCN nanocages was confirmed by FT-IR measurement (Fig. 2 inset). MBN nanocage exhibits the peaks centered at 1375 and 800  $\text{cm}^{-1}$  in the spectrum which are attributed to the in-plane B-N stretching and out-of-plane B-N-B vibrations of h-BN, respectively, revealing the presence of B-N bonds in the wall structure.<sup>21</sup> No vibration peak associated with C and O is observed, confirming again the purity of the sample. On the other hand, two more additional bands are observed together with the above bands centered at 1100  $\text{cm}^{-1}$  and 2340  $\text{cm}^{-1}$  for MBCN which are attributed to B-C and  $\text{-C}\equiv\text{N}$  stretching, respectively.<sup>21</sup> The Raman spectra of MBN and MBCN (see Fig. S3 in ESI) also support the formation of h-BN. The peak at 1352  $\text{cm}^{-1}$  is appeared for MBN which is caused by the B-N bond vibration and phonon dispersion within a plane.<sup>22</sup> Interestingly, MBCN exhibits two peaks centered at 1345 and 1580  $\text{cm}^{-1}$  which correspond to the D and G bands of B-C-N compounds, respectively. Similar results were also observed by other researchers for BCN nanotubes, confirming the highly crystalline nature.<sup>22</sup>

In order to further confirm the mesoporosity in MBN and MBCN, the materials were analyzed by nitrogen adsorption and the results are shown in Fig. 3. The nitrogen adsorption isotherm of both the samples are found to be type IV and exhibit H1 type broad hysteresis loop, which is typical of mesoporous solids. Interestingly, mesoporous BN nanocage registered the surface area of 945  $\text{m}^2/\text{g}$  and the specific pore volume of 1.05  $\text{cm}^3/\text{g}$  which is almost two times higher than those of the previously reported MBN and 20 times higher than the nonporous BN.<sup>16</sup> These values are quite remarkable, which was possible because of the combination of 3D structure and cage type pores in the BN. It is interesting to note that the specific surface area and pore volume of the MBCN nanocage are 1023  $\text{m}^2/\text{g}$  and 1.3  $\text{cm}^3/\text{g}$ , respectively, which are much higher than those of MBN. This could be due to the lower reaction temperature and the presence of less dense C in the BN matrix. It should also be noted that the capillary condensation for both the samples is observed at the similar relative pressure of the carbon nanocage, which gives a similar pore diameter and confirms the successful replication of the template via elemental substitution method (Fig. 3 inset). However, the specific surface area and the specific pore volume of the MBN and MBCN are lower than those



of the template (SA: 1600  $\text{m}^2/\text{g}$ ; PV: 2.1  $\text{cm}^3/\text{g}$ ).<sup>17</sup>

Fig. 3 Nitrogen adsorption isotherms of MBN and MBCN nanocages (inset: BJH adsorption pore size distribution of MBN and MBCN)

## Conclusions

In summary, we have demonstrated a low temperature synthesis of novel mesoporous cage type BN and BCN spheres in micrometer range using carbon nanocage with 3D porous structure and spherical morphology as a template and boron trioxide as a boron source through elemental substitution method. The combination of the spherical morphology and 3D template was effective to prepare MBN and MBCN nanocages with remarkable surface area and pore volumes which are 20 times higher than those of the nonporous BN and BCN samples. In addition, the samples possess highly crystalline wall structure with ordered spherical morphology and uniform pore size distribution, confirming the elemental substitution process. We believe that these remarkable textural parameters together with the spherical morphology in BN and BCN could open the door for many applications. It is further anticipated that this novel strategy could apply to many other processes to create novel BN and BCN nanostructures with different structures and morphology.

## Notes and references

<sup>a</sup>AIBN, The University of Queensland, Brisbane 4072, QLD, Australia. Fax: +61-7-3346-3973; Email: a.vinu@uq.edu.au

<sup>b</sup>International Centre for Materials Nanoarchitectonics, National Institute for Materials Science, Tsukuba 305-0044, Ibaraki, Japan

<sup>c</sup>Department of Chemistry and Nano Science, Ewha Womans University, Seoul, South Korea

<sup>d</sup>Department of Chemistry, King Saud University, Riyadh, Saudi Arabia.

Electronic Supplementary Information (ESI) available: [Higher angle XRD pattern and Raman spectra of MBN and MBCN nanocages are included in the supporting information]. See DOI: 10.1039/c000000x/

## Acknowledgement

This work was partially supported by the Ministry of Education, Culture, Sports, Science and Technology (MEXT) under the Strategic Program for Building an Asian Science and Technology Community Scheme and World Premier International Research Center (WPI) Initiative on Materials Nanoarchitectonics, MEXT, Japan. One of the authors A. Vinu thanks Australian Research Council for the award of Future Fellowship and AIBN for the start-up grant. A.V Also acknowledges the financial support from King Saud University.

1. R.T. Paine and C.K. Narula, *Chem. Rev.*, 1990, **90**, 73.
2. R. W. Rice, J. R. Spann, D. Lewis, Z. Coblentz, *Ceram. Sci. Eng. Proc.*, 1984, **5**, 614.
3. S. J. Yoon and J. Jha, *J. Mater. Sci.* 1995, **30**, 607.
4. H. Huang and E.E. Remsen, *J. Am. Chem. Soc.*, 1999, **121**, 3805.
5. E. Mathlowitz, J. S. Jacob, Y. S. Jong, G. P. Carino, D. E. Chickering, P. Chaturvedl, C. A. Santos, K. Vijayaraghavan, S. Montgomery, M. Bassett and C. Morrell, *Nature*, 1997, **386**, 410.
6. Y. D. Yin, Y. Lu, B. Gates and Y. N. Xia, *Chem. Mater.*, 2001, **13**, 1146.
7. M. Ohmori and E. Matijevic, *J. Colloid Interface Sci.*, 1992, **150**, 594.
8. C. Tang, Y. Bando and D. Golberg, *Chem. Commun.*, 2002, 2826.
9. a) B. Toury, P. Miele, D. Cornu, H. Vincent and J. Bouix, *Adv. Funct. Mater.*, 2002, **12**, 228. b) Y. L. Gu, M. T. Zheng, Y. L. Liu and Z. L. Xu, *J. Am. Ceram. Soc.*, 2007, **90**, 1589. c) G. L. Wood, J. F. Janik, M. Z. Visi, D. M. Schubert and R. T. Paine, *Chem. Mater.*, 2005, **17**, 1855. d) G. L. Wood, R. T. Paine, L. Gary, R. T. Paine and T. Robert, *Chem. Mater.*, 2006, **18**, 4716. e) L. Shi, Y. L. Gu, L. Y. Chen, Y. T. Qian, Z. H. Yang and J. H. Ma, *J. Solid State Chem.*, 2004, **177**, 721. f) T. Oku, T. Hirano, M. Kuno, T. Kusunose, K. Niihara and K. Suganuma, *Mater. Sci. Eng. B*, 2000, **74**, 206. g) L. Boulanger, B. Andriot, M. Cauchetier and F. Willamine, *Chem. Phys. Lett.*, 1995, **234**, 227. h) F. Banhart, M. Zwanger and H. J. Muhr, *Chem. Phys. Lett.*, 1994, **231**, 98. i) W. Q. Han, Y. Bando, K. Kurashima and T. Sato, *Jpn. J. Appl. Phys.*, 1999, **38**, L755.
10. D. A. Lindquist, T. T. Kostas, D. M. Smith, X. M. Xiu, S. L. Hietala and R. T. Paine, *J. Am. Ceram. Soc.*, 1991, **74**, 3126.

11. E. A. Pruss, G. L. Wood, W. J. Kroenke and R. T. Paine, *Chem. Mater.* 2000, **12**, 19.
12. G. L. Wood, J. F. Janik, E. A. Pruss, D. Dreissig, W. J. Kroenke, T. Habereeder, H. Noth and R. T. Paine, *Chem. Mater.*, 2006, **18**, 1434.
13. S. Yuan, L. Zhu, M. Fan, X. Wang, D. Wan, S. Peng and H. Tang, *Mater. Chem. Phys.*, 2008, **112**, 912
14. C. T. Kresge, M. E. Leonowicz, W. J. Roth, J. C. Vartuli and J. S. Beck, *Nature*, 1992, **359**, 710.
15. P. Dibandijo and L. Bois, *Adv. Mater.*, 2005, **17**, 571.
16. A. Vinu, M. Terrones, D. Golberg, S. Hishita, K. Ariga and T. Mori, *Chem. Mater.*, 2005, **17**, 5887.
17. A. Vinu, M. Miyahara, V. Sivamurugan, T. Mori and K. Ariga, *J. Mater. Chem.*, 2005, **15**, 5122.
18. M. Hubacek and T. Sato, *J. Solid state Chem.*, 1995, **114**, 258.
19. J. Thomos, N. E. Weston and T. E. O'Connor, *J. Am. Chem. Soc.*, 1962, **84**, 4619
20. D. Golberg, Y. Bando, L. Bourgeois, K. Kurashima and T. Sato, *Appl. Phys. Lett.*, 2000, **77**, 1979.
21. H. Sachdev, R. Haubner, H. Noth and B. Lux, *Diamond Relat. Mater.*, 1997, **6**, 286.
22. C. Y. Zhi, X. D. Bai, and E. G. Wang, *Appl. Phys. Lett.*, 2002, **80**, 3590.

A low temperature synthesis of novel mesoporous BN and BCNs with cage type porous structure, high surface area, and spherical morphology using carbon nanocage has been reported.

